International Journal of Energy Science (IJES) Volume 3 Issue 5, October 2013 www.ijesci.org
DOI: 10.14355/ijes.2013.0305.05

Dynamic Modeling and Analysis of a Remote Hybrid Power System with Pumped Hydro Storage

Md. Rahimul Hasan Asif[1], Tariq Iqbal[2]

[1,2]Faculty of Engineering and Applied Science, Memorial University of Newfoundland
St. John's, NL A1C 5S7, P.O. Box 4200, CANADA

[1]mrha46@mun.ca; [2]tariq@mun.ca

Abstract

In this research, dynamic modeling of a remote hybrid power system and feasibility of a pumped hydro storage system is presented. Current hybrid system in Ramea, Newfoundland has an electrolyzer, storage and hydrogen generator system. This research proposes a pumped hydro storage as a replacement to the hydrogen system. Detailed MATLAB-Simulink modeling has been done for every component of the Ramea hybrid power system. Incorporation of a pumped hydro system and some lead acid batteries will eliminate the low turn around efficiency of the electrolyzer and hydrogen generator system. The system dynamic model presented here is fast, accurate and includes dynamic and supervisory controllers. The proposed real time supervisory controller algorithm observes the available surplus/missing power in the system and regulates pump/turbine and charging/discharging of the battery bank to maintain a stable system frequency. This paper presents dynamic model, supervisory controller design and algorithm, six case studies and detailed simulation results.

Keywords

Dynamic Modeling; Wind-diesel systems; Pumped Hydro Storage; Hybrid Power Systems; Renewable Energy

Introduction

Ramea, a small island located off the south coast of Newfoundland, Canada, in 2004, was selected as the first pilot project site for a Wind-Diesel hydrogen hybrid power system which was led by the Newfoundland and Labrador Hydro. The main objective of this project was to demonstrate substantial improvement of energy efficiency and reliability after incorporating Wind-Diesel Integrated Control System (WDICS) in the island's grid which can reduce the use of diesel power by hosting green renewable wind energy in remote and isolated location. This wind-diesel pilot system generates almost 1million kWh of electricity and offsets nearly 750 tons of greenhouse gas emissions per annum [1] [2].

Wind energy system in Ramea has six 65 kW Windmatic 15 s and three 100k W NorthernPower100 wind turbines (WT). Three 925 kW Diesel engine generators (DEG) are used as the main power source. A Hydrogen Electrolyzer and Storage (HES) and a 250 kW Hydrogen Powered Generator (HPG) have been installed to increase the renewable energy penetration. When wind power generation exceeds the load, the electrolyzer produces hydrogen from water electrolysis which is stored in the storage tanks. And when harnessed wind power is inadequate to supply the total load, the stored hydrogen is fed into a HPG as a fuel which delivers electricity to the grid and maintains the stability [2]. This HES system produces hydrogen at 70% efficiency and HPG generates electricity at less than 35% efficiency. Overall, it gives a poor turn around conversion efficiency that is less than 25% [3]. Ramea system has many operational issues due to its complexity. So far, it never operated as designed. Detailed information, analysis and dynamic simulation for the optimal size and site selection of a pumped hydro storage (PHS) system replacing the HES and HPG has been presented in Ref. [4]. It has been explained that almost 37% renewable energy fraction can be attained using a 150 kW PHS system with a 3932 m^3 water reservoir at 63 m height on top of 'Man of War' hill [4]. Topographical map of that hill shows that it has 2000 m^2 of area to build a 2 m height hydro storage reservoir. In Ref. [4] only 24 s of dynamic simulation has been presented as it took days of computer time to simulate 1 min of system operation. Moreover, the simulation didn't converge in the time period of 11 s to 16 s. Simple first order modeling of every system component can considerably reduce the simulation time, make the

DOI: 10.14355/ijes.2013.0305.05

analysis easier and give fairly accurate solutions. Research [5] shows the system stability of a self-governing hybrid renewable power generation and storage system connected with isolated loads by time-domain simulations. As storage subsystems, that hybrid system has a battery bank (BB) and a flywheel system. Three mathematical models have been investigated for three different sets of operating points and disturbance conditions. But the presented mathematical subsystems are too simple where nonlinear efficiency, friction and response time are ignored and there is no controller in the model. The real challenge is to model practical subsystems with simple first order models juxtaposing all efficiencies, dynamic frictions, different time constants related to the subsystem parameters.

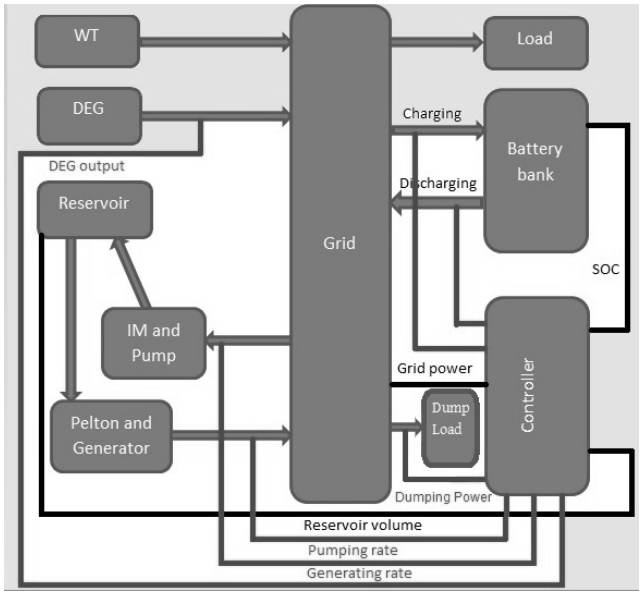

FIG. 1 BLOCK DIAGRAM OF RAMEA HYBRID POWER SYSTEM WITH A PROPOSED PUMPED HYDRO STORAGE SYSTEM, BATTERY BANK AND DUMP LOAD

A simple, fast and novel method has been introduced in this research work to simulate system dynamics of Ramea hybrid power system with a proposed PHS. A block diagram of Ramea hybrid power system is shown in FIG. 1 Some system details may be found in [6]. A BB has been used to supply or store the intermittent power as induction motor (IM) and centrifugal pump (CP) or turbine and generator require some time to reach a certain rated operating point and have larger time constant than a battery bank. A controllable dump load (DL) has also been used to dump the excess power. The presented model has PID controllers with all its subsystems. Characteristic data and parameters of the aforementioned WTs and DEG used in Ramea hybrid system are taken from the respective manufacturers. All other subsystem models e.g. CP, Pelton Wheel Turbine (PWT), BB have been created using first principle and data obtained from manufactures. In this study, dynamic models with 1st order transfer functions (TF) are considered. Simulations have been done for one day (86400s) for six extreme cases. Detailed results and analyses are presented in the later part of this paper.

Dynamic Modeling

Wind Speed Data

Wind speed data (1 Hz) from the Prince Edward Island (PEI), Newfoundland, Canada is used. Average value of the data was adjusted to represent wind speed at Ramea. Two wind speed average have been considered here e.g. 2.9 m/s and 13.75 m/s.

Load Data

Ramea load data for two days is used from Ref. [4]. Two 24 hour load curves are used from the data array with averages of 303 kW and 800 kW.

Wind Turbine Model

WT power curves have been collected from the corresponding manufacturers. Power curve data was fitted with a 6th order polynomial.

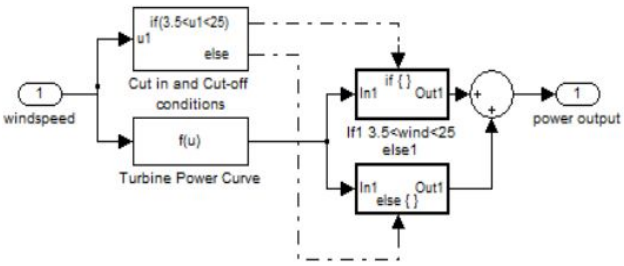

FIG. 2 WIND TURBINE POWER CURVE AND LIMITING CONDITIONS

As shown in FIG. 2 necessary cut in and cut out wind speed conditions have been applied in the WT model. Wind turbine time, constants are used following the equation from the Ref. [7]:

$$H_{WT} \cong 1.87 * P_{WT}^{0.0597} \quad (1)$$

In Eq. (1) H_{WT} is the mechanical inertia time constant and P_{WT} is the power of the WT in watts. So calculation gives 3.6 s for 65 kW Windmatic 15 s [8] and 3.7 s for 100 kW Northern Power 100 [9]. In FIG. 3 all WTs, load

DOI: 10.14355/ijes.2013.0305.05

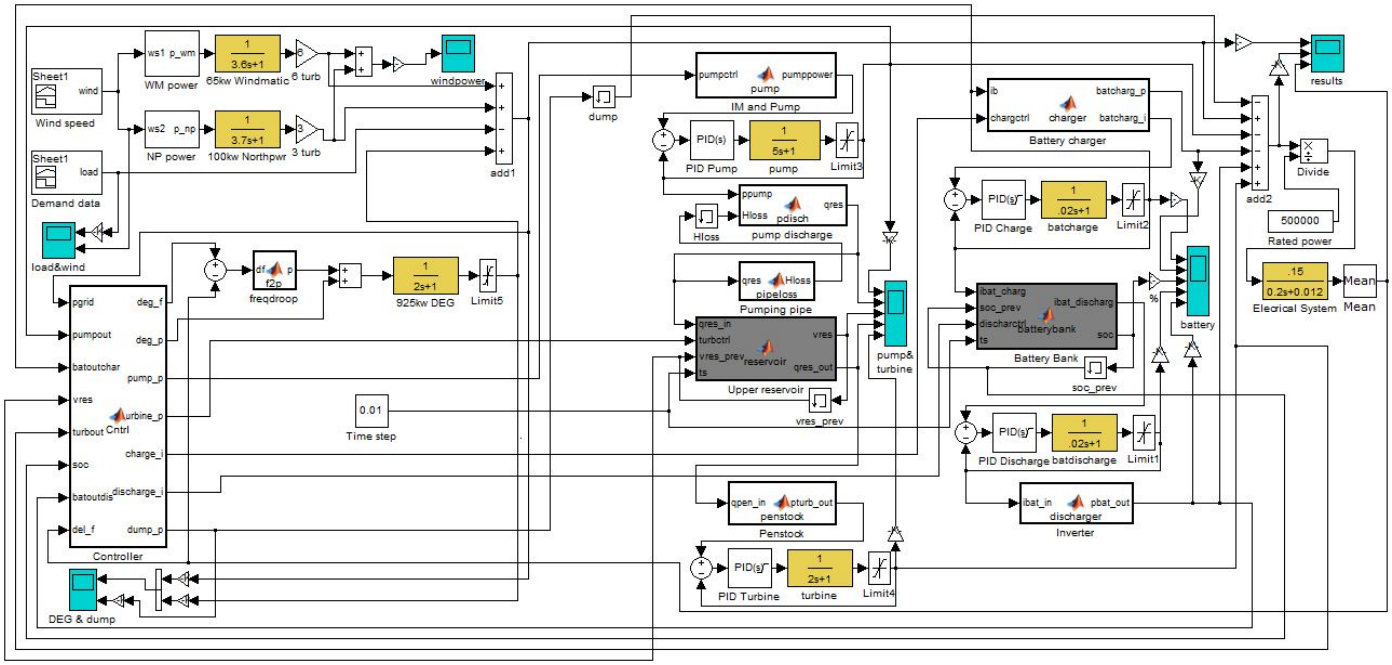

FIG. 3 SIMULINK - MATLAB EMBEDDED FUNCTION BLOCKS BASED DYNAMIC MODEL OF RAMEA HYBRID POWER SYSTEM WITH PUMPED HYDRO STORAGE, BATTERY BANK AND DUMP LOAD

demand and varying DEG output are connected with an adder 'add1'. Output of 'add1' represents the power available or lack in the grid which has to be managed by the PHS or BB.

Diesel Engine Generator Model

DEG in Ramea has a rated output of 925 kW. There are three DEG but only one is used at a time. A DEG can be operated down to 30% of its rated output i.e. the DEG can operate from 300 kW to 925 kW. However, a DEG always keeps running at 300 kW (a minimum), whatever the case, to maintain a stable system frequency. Time constant of DEG is taken as it is used in Ref. [5] so TF_{DEG} = 1/(2s +1). This value has been verified from the datasheet of a DEG of almost same rating. The acceleration time constant of DEG is calculated by the following Eq. (2),

$$J = S_n \frac{T_{DEG}}{\omega_n^2} \quad (2)$$

Here, J is the moment of inertia; ω_n is the rated angular velocity which equals $2\pi f$; S_n is the DEG nominal apparent power; T_{DEG} is the acceleration time constant rated to S_n. In the datasheet of the DEG, J = 20 kg.m^2. That results in the acceleration time constant of DEG of $T_{DEG} \cong 2$ s. With this time constant, this DEG needs about 10 s to reach its steady state value.

Frequency droop curve has been introduced considering that this DEG has a $\Delta P/\Delta f$ ratio of 300 kW/1Hz. The MATLAB code used here is,

```
dpu = 1 - (62 - (df + 60))/2
```
(3)

In Eq. (3) `dpu` is per unit excess power that will be injected to balance out the frequency deviation, `df` in the grid.

Induction Motor and Centrifugal Pump Model

Considering their individual characteristics, IM and CP are modeled together in a block (IM and Pump block in FIG. 3). The CP takes relatively large time to respond to a sudden change compared to an IM. Comparing the starting time of a combination of IM and CP from Ref. [10], a 4000 hp – 1000 rpm pumping system takes approximately 2.5 minutes to reach its rated output. Here it has been assumed that a 200 hp pumping system needs 30 s to settle down its steady state. Therefore, transfer function of this block is TF_{CP} = 1/(5s +1). K_P = 0.4732, K_I = 0.3391 and K_D = 0 are used in PID controller of CP. Built in tuner of Simulink PID block has been used for this block as well as rest of the blocks in this model to determine suitable controller parameters. Efficiencies of IM and CP are considered as 95% and 80% respectively, which gives a total efficiency of 75%. Eq. (4) is used in MATLAB code to determine `qres` = pumping water flow to reservoir.

```
qres = (ppump*pmeff)/(hres+Hloss)*dens*g
```
(4)

Here, `ppump` = power delivered to the pumping system which can vary from 30% to 100% of the rated output e.g. 100 kW to 300 kW; `pmeff` = 75%; `hres` = 63 m (height of the reservoir); `Hloss` = penstock friction loss;

DOI: 10.14355/ijes.2013.0305.05

dens = 1000 kgm^{-3} and g = 9.81 ms^{-2}.

Penstock Model

Penstock is designed as Lpipe = 70 m in length and Dpipe = 0.3 m in diameter. Reynolds number is selected assuming that water flow is laminar inside the pipe. A minor loss coefficient for water meter is used here as klossco which is taken equal to 7 [11].

```
Velowaterpump = qres/Apipe; %water velocity
Re = 2000; %Reynolds number
flam = 64/Re; %Darcy Friction Factor for laminar flow
hpipefric=
(8*flam*Lpipe*qres^2)/(g*π^2*Dpipe^5); (5)
hlossmeter = klossco*(Velowaterpump^2)/(2*g);
Hloss = hpipefric + hlossmeter;
```

Eq. (5) used here is Darcy–Weisbach equation for friction inside the penstock [12]. Here Hloss is calculated in each step for new qres.

Water Reservoir Model

The proposed water reservoir has a total volume of 4000 m^3. In simulations, initial volume is considered as 2000 m^3. Pump action will be stopped if water volume exceeds 3950 m^3 and turbine action will be terminated if water volume goes below 150 m^3. Total water volume in the reservoir can be determined from water flows in both ways or from the height of water in the reservoir (see upper reservoir block in FIG. 3).

Turbine Model

A 150 kW PWT has been used here which has very good partial flow efficiency as shown in FIG. 4 [13]. The blue curve here is for a twin jet setup. Synchronous generator and PWT are modeled together using a combined efficiency of 70% and time constant of 2 s as DEG. TF of this block is $TF_{TURB} = 1/(2s+1)$. $K_P = 0.4732$, $K_I = 1.6955$ and $K_D = 0$ are used in PID controller of PWT (turbine block in FIG. 3). The power output of the turbine generator block is as in Eq. (6)

```
pturb_out = qpen_in*hres*dens*g*turbeff (6)
```

Here, pturb_out = turbine output power, qpen_in = incoming water flow to the turbine and turbeff = 70% as turbine efficiency.

Battery Bank Model

In an isolated grid BB used as storage provides fast response which makes them favorable to improve power quality and gains system reliability. A bank of 300 batteries has been used here each having a capacity of 200 Ahr. Total 15 branches are connected in

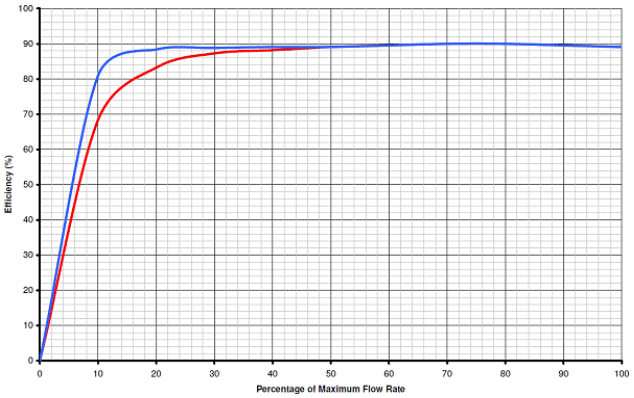

FIG. 4 PART FLOW EFFICIENCY OF A PELTON WHEEL TURBINE

parallel where each branch consists of 20 batteries in series delivering a DC battery bus voltage of 240 V. A charging and a discharging block have been created to control the current and monitor the State of Charge (SOC) of the battery. A SLA battery should not be discharged when SOC goes down to 40%. Total coulomb capacity can be determined from the calculations below in (7), (battery bank block in FIG. 3)

Total cap = individual cap * 3600 * no. of branch (7)

= 200*3600*15 = 10800000C (at 100% SOC)

So the BB operates from 100% SOC to 40% SOC (4320000C). For charging current, a maximum 10% of the individual capacity will be allowed as in (8) where charge_i = total charging current, ind_cap = individual capacity and nbat_para = no. of branches.

```
charge_i = 0.1 * ind_cap * nbat_para (8)
discharge_i = 0.33 * ind_cap * nbat_para (9)
```

A maximum of 72 kW surplus power can be utilized to charge the BB almost instantaneously. For a maximum power shortage of 234 kW can be supplied from the BB by discharging it to 'one third of the individual capacity'. In (9) discharge_i = total discharging current. In this model, initial SOC is chosen as 70% which is equivalent to 7560000 C. While discharging, battery bank can be discharged at any rate below 0.33 CA but that will affect the effective capacity of battery following the 'Peukert's law'.

$$It = C\left(\frac{C}{IH}\right)^{k-1} \quad (10)$$

Here, '*It*' is the effective capacity at discharge rate of *I*, *H* is the rated discharge time, in (hours), *k* is the

DOI: 10.14355/ijes.2013.0305.05

Peukert constant which is 1.2 for SLA battery. Along with this in this model, the combined efficiency of battery and converters is considered as 80%. Eq. (11) is used to calculate the power delivered (`pbat_out`) by the battery where `v_bat` = 240V, `ibat_in` = total discharging current and `bateff` = 80%.

```
pbat_out = v_bat * ibat_in * bateff        (11)
```

TF of Battery Discharge block (FIG. 3) is $TF_{BB} = 1/(0.02s+1)$. As SLA battery has a very fast response in the range of milliseconds [14], here modeled BB takes less than 100 ms to reach steady state. Coefficients for the PID controller of this block are K_P = 0.0001, K_I = 213617.933 and K_D = 0. The BB will provide power while mechanical subsystems start up.

Dump Load Model

A 1 MW (maximum) controllable dump load has been used to curtail the excess power from the grid while the wind speed is considerably high and/or the load demand is low. Maximum power dissipation in the dump load is 800 kW (in the case 2 where wind speed is high and load is low). A PWM controller can be used to dump the surplus power from the grid to the dump load. The dump load help reduce the frequency spikes in the grid.

Model of the Electrical System

The system inertia constant M and load-damping constant D have been used the same as in Ref. [5]. The gain has been changed from 1.0 to 0.15 as 1.0 makes the system too sensitive. TF of the electrical system has been considered as $TF_{ELEC} = 0.15/(0.2\ s+0.012)$. Therefore, 0.05 pu power deviation will cause 0.01 pu or 0.6 Hz frequency deviation (see electrical system block in FIG. 3).

Supervisory Controller

PID controllers have been used to control all individual subsystems. To determine the optimum coefficients for the PID controllers, Simulink built in PID tuner has been used. Limiters have been used to clip all out of range values. A simple flowchart of the algorithm used in this model as the supervisory controller is shown in FIG. 5. It is shown as a block 'controller' in the FIG. 3. DEG has the least priority to take control. Pump and Pelton wheel operate with the highest priority as per the requirement and BB compensates for the intermittent deviations due to the inertial delay of rotating mechanical devices. In each step, supervisory controller keeps measuring the reservoir water volume, SOC and the grid power. When DEG takes control, a differential block measures the frequency deviation from the set value and according to the frequency droop characteristics curve of the DEG which adjusts its output power.

Results: Six Case Studies

For different conditions of wind speed and load, six cases are proposed in Table 1. These six cases cover possible normal and extreme operation of the hybrid power system.

TABLE 1 SIX DIFFERENT CASES OF LOAD AND WIND SPEED

Case	Load	Wind speed
1	Low (200kW to 330kW)	Low (0m/s to 9m/s)
2	Low (200kW to 330kW)	High (10m/s to 20m/s)
3	High (590kW to 990kW)	Low (0m/s to 9m/s)
4	High (590kW to 990kW)	High (10m/s to 20m/s)
5	Abrupt load change (500kW to 700kW at 200s and vice versa at 700s)	Steady in midrange (5m/s)
6	Steady in midrange (500kW)	Abrupt wind speed change (8m/s to 11m/s at 200s and vice versa at 700s)

Simulation of the developed system model shown in FIG. 3 has been done for one day i.e. 86400 s. Site wind speed data and load data have been used [4]. Data is from the year 2001. Inspecting site wind speed data and load data, the lowest 24 hours average load was found to be 303 kW on September 3, 2001 which is referred to as 'Low load' in this paper. Load varies between 200 kW to 330 kW from 12:00:00AM to 11:59:59PM. And the highest load found in the year of 2001 is 800 kW on December 29, 2001 where load varied from 590 kW to 990 kW throughout the day. This is referred to as 'High load' in this paper.

Observing all daily average of wind speed data, it has been found that on September 17, 2001 the lowest daily average of wind speed was recorded which was 2.9 m/s and wind speed stayed between 0 m/s to 9 m/s. This is referred to here as 'Low wind'. The highest daily average wind speed has been found to be 13.75 m/s on February 26, 2001 where it varied between 10 m/s to 20 m/s. This wind speed pattern is referred to as 'High wind' in this paper. As an abrupt change of load, it is assumed that for a 1000 s time period load changes to 700 kW from 500 kW at t=200 s and drops

DOI: 10.14355/ijes.2013.0305.05

to 500 kW again at t=700 s while wind speed stays steady at 5 m/s. On the other hand, abrupt change of wind speed has been considered as a rise to 11 m/s from 8 m/s at t=200 s and again dropping back to 8 m/s at t=700 s. For this change, the load has been assumed to be constant at 500 kW. Results for all six case studies with theses extreme conditions are presented below.

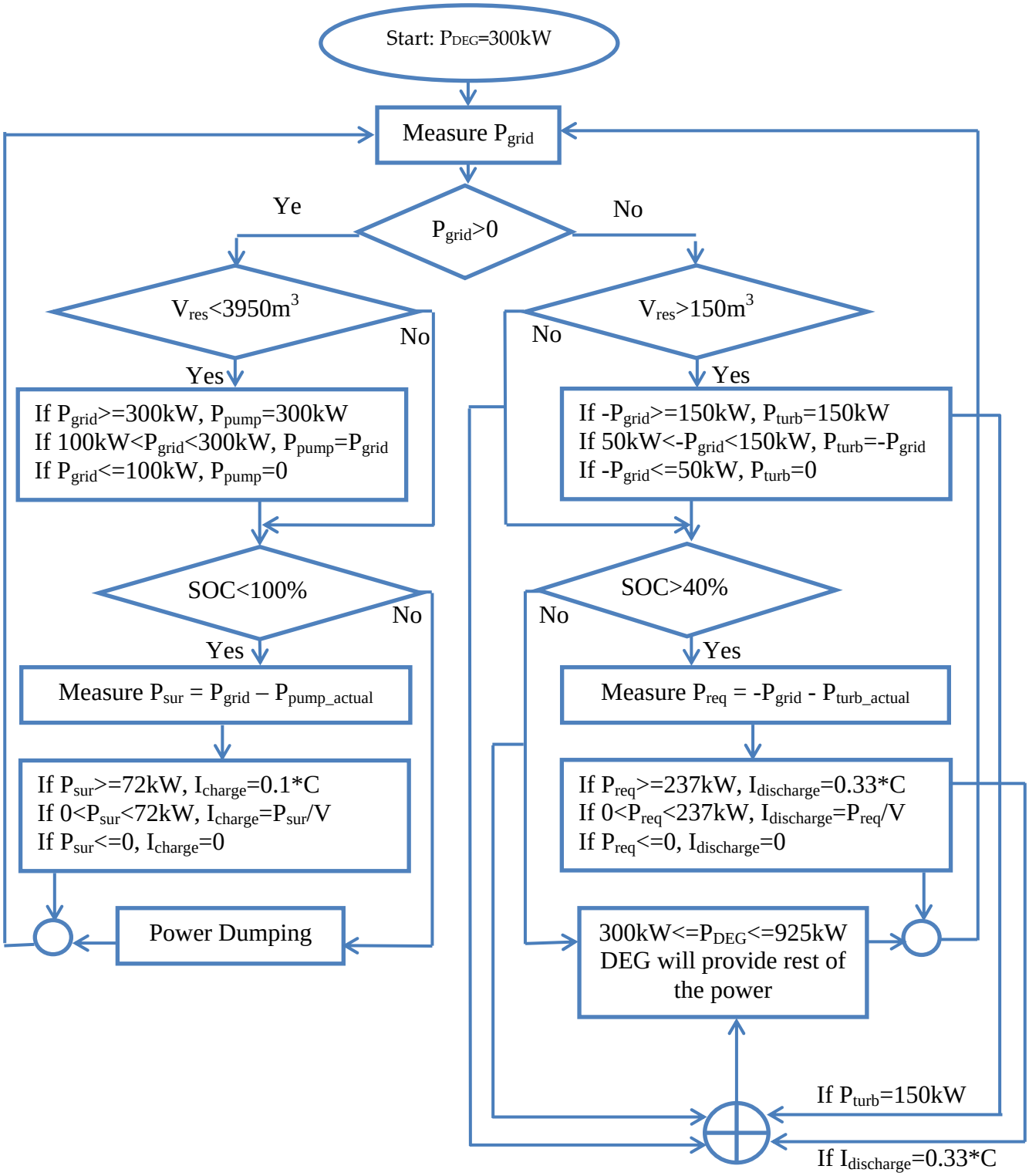

FIG. 5 SIMPLE FLOWCHART OF THE ALGORITHM USED AS SUPERVISORY CONTROLLER

DOI: 10.14355/ijes.2013.0305.05

Case 1: Low Load and Low Wind

In Case 1, Low load and low wind speed have been used as inputs to the dynamic model and system outputs are observed.

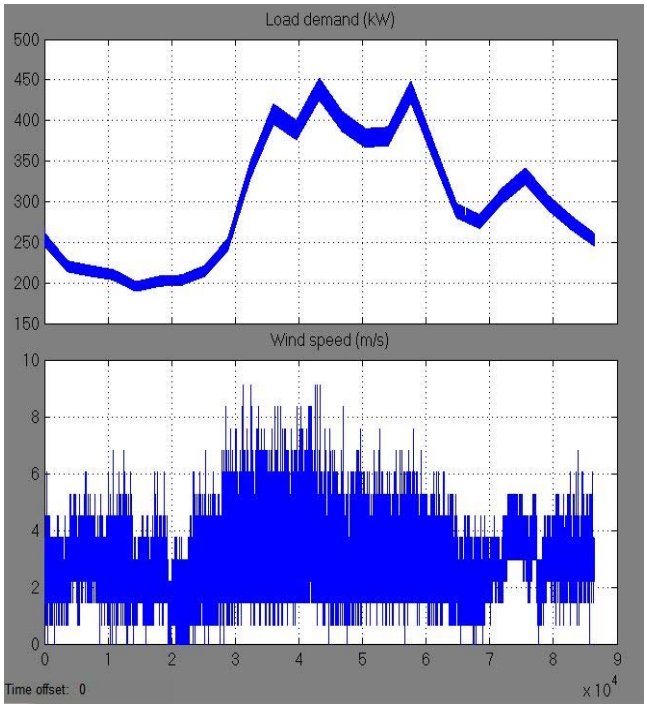

FIG. 6 LOAD DEMAND (kW) AND WIND SPEED (m/s) DATA FOR THE CASE 1

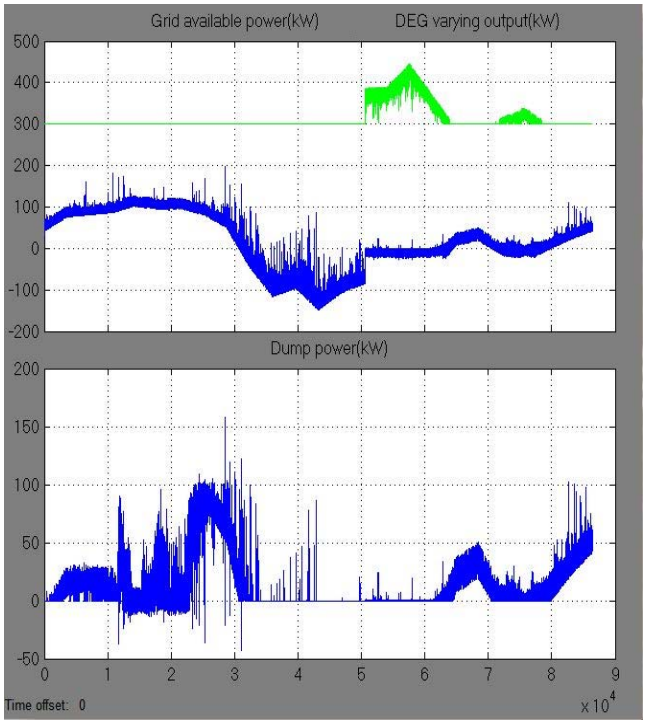

FIG. 7 IN TOP FIGURE, THE GRID AVAILABLE POWER (kW) AND DEG VARYING OUTPUT (kW) (WITH A MINIMUM 300kW VALUE) IS SHOWN AND IN THE LOWER FIGURE DUMP POWER (kW) IS SHOWN FOR THE CASE 1

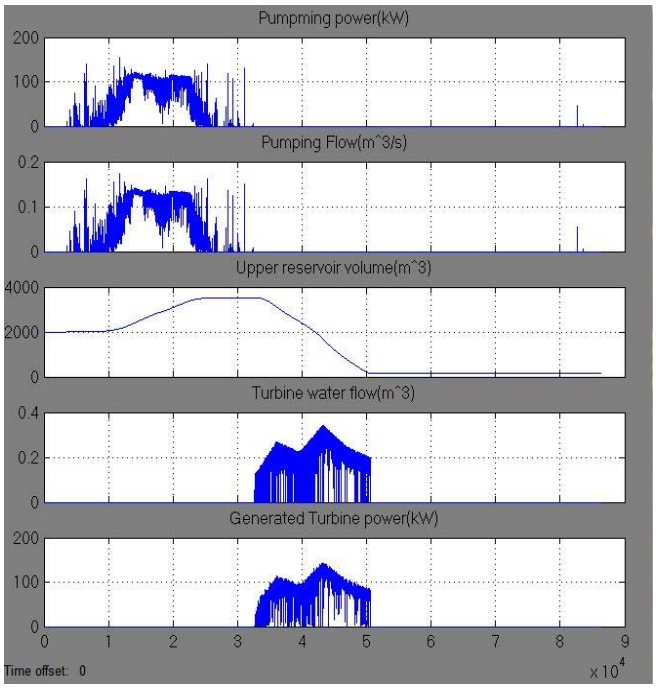

FIG. 8 PUMP POWER CONSUMPTION (kW), PUMP WATER FLOW (m^3/s), THE UPPER RESERVOIR WATER VOLUME (m^3), TURBINE WATER FLOW RATE (m^3/s) AND THE TURBINE GENERATED POWER (kW) FOR THE CASE 1

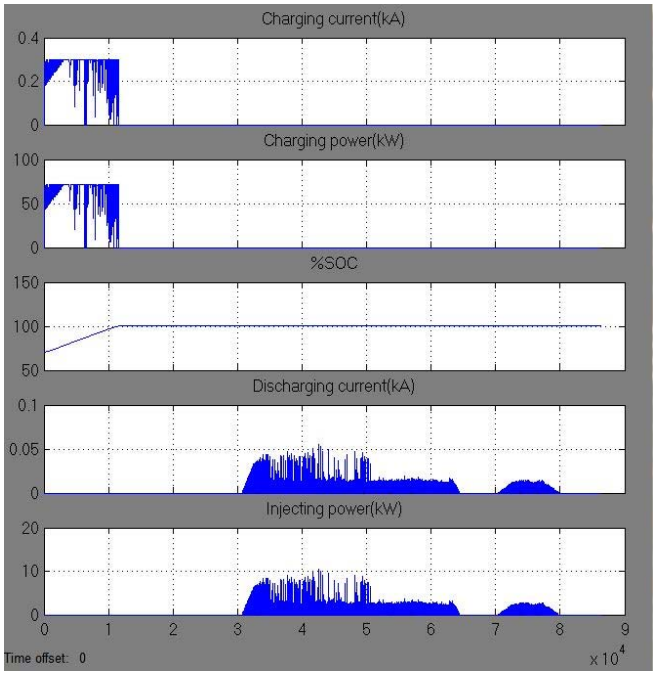

FIG. 9 BB CHARGING CURRENT (kA), CHARGING POWER (kW), PERCENTAGE OF STATE OF CHARGE, DISCHARGING CURRENT (kA) AND THE POWER TO THE GRID (kW) DUE TO THE DISCHARGING OF THE BATTERY ARE SHOWN FOR THE CASE 1

From FIG. 6 to FIG. 10, it can be observed that in the first 30000 s load was very low so CP and BB charger worked to store the excess energy. From 30000 s to 50000 s, load was increasing and PWT and BB delivered the necessary power. After 50000 s, reservoir

DOI: 10.14355/ijes.2013.0305.05

is empty so DEG takes control and supplies a maximum of 450 kW for some time. System frequency remains almost stable that day. A sudden frequency dip of 1.3 Hz is observed in FIG. 10 when load is increasing rapidly after t = 30000 s and PWT responds slowly. Such a frequency dip is acceptable in remote hybrid power systems. This case study indicates that the developed model and supervisory controller is capable of correctly simulating the hybrid power system. The transients observed in these figures are not instantaneous rather slow variations. The x-axes cover a whole day simulation (86400 s) so these spikes are basically steady variations lasting minutes. In FIG. 11, a zoomed result from 57700 s to 57800 s has been shown.

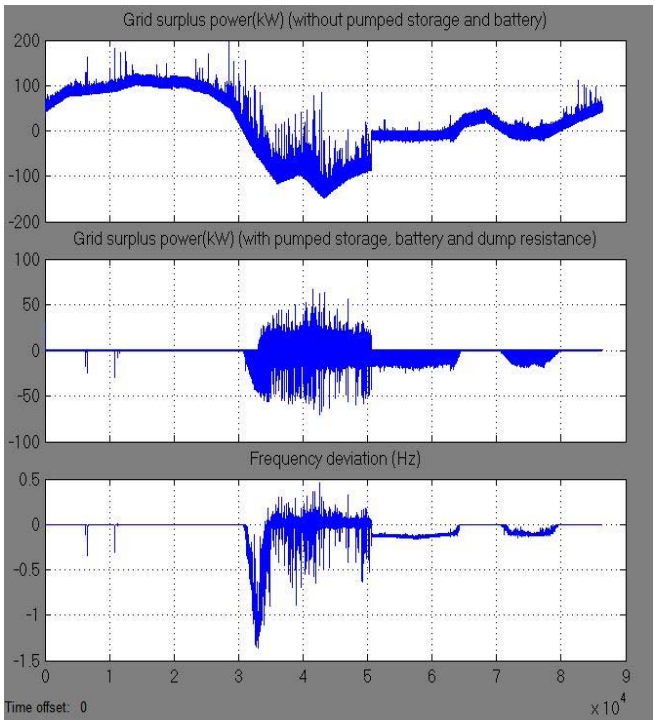

FIG. 10 GRID SURPLUS POWER (kW) WITH AND WITHOUT PUMPED STORAGE, BATTERY AND DUMP LOAD AND THE RESULTANT FREQUENCY DEVIATION FOR THE CASE 1

Case 2: Low Load and High Wind

In case 2, a low load and high wind speed have been used in the dynamic model to observe the system outputs and responses. FIG. 12 shows the selected data. Daily load cycle and random variation is shown in the top section of FIG. 12. From FIG. 13 to FIG. 16 it can be observed that as wind is high and load is low, the water reservoir and BB become fully charged in the first 8000 s and 10000 s respectively. After that, all the excess power goes to the dump load. The maximum power dissipation in the dump load is 800 kW. System frequency is totally stable for all time as it is maintained by the diesel. These results also show that the developed model is capable of correctly simulating the complex Ramea hybrid power system.

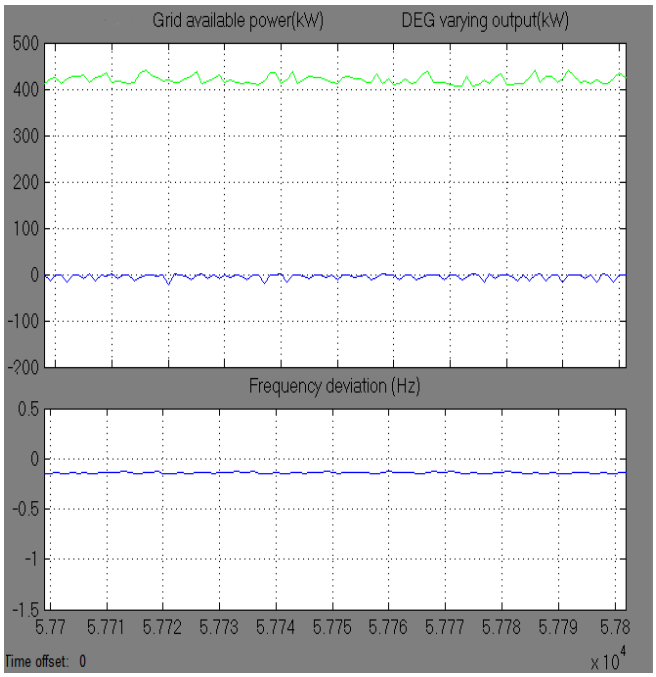

FIG. 11 SIMULATION RESULT HAS BEEN ZOOMED FROM 57700s TO 57800s TO SHOW THE TRANSIENTS. IN TOP FIGURE, THE GRID AVAILABLE POWER (kW) AND DEG VARYING OUTPUT (kW) IS SHOWN AND IN THE LOWER FIGURE THE RESULTANT FREQUENCY DEVIATION IS SHOWN FOR THE CASE 1

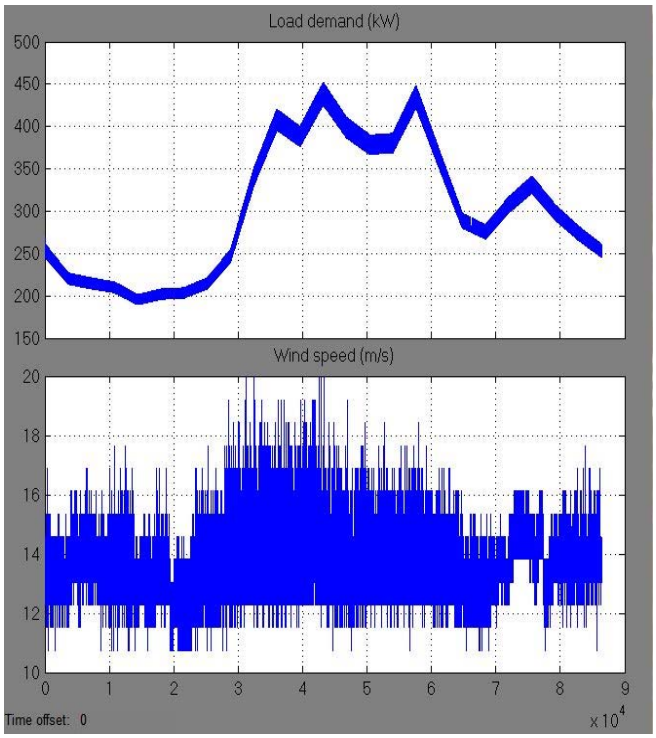

FIG. 12 LOAD DEMAND (kW) AND WIND SPEED (m/s) DATA FOR CASE 2

DOI: 10.14355/ijes.2013.0305.05

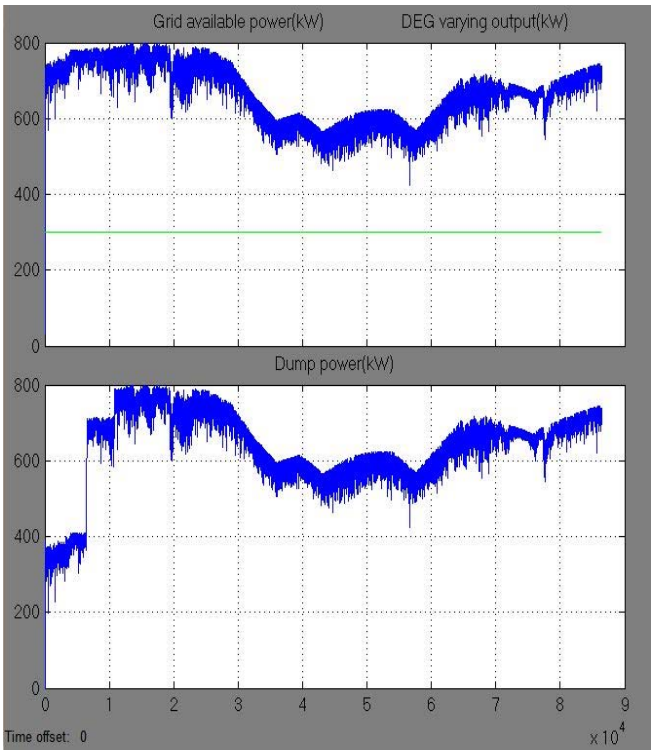

FIG. 13 IN THE TOP PART, GRID AVAILABLE POWER (kW) AND DEG OUTPUT (kW) (WITH FLAT 300kW VALUE) ARE SHOWN AND IN THE LOWER PART DUMP POWER (kW) IS SHOWN FOR THE CASE 2

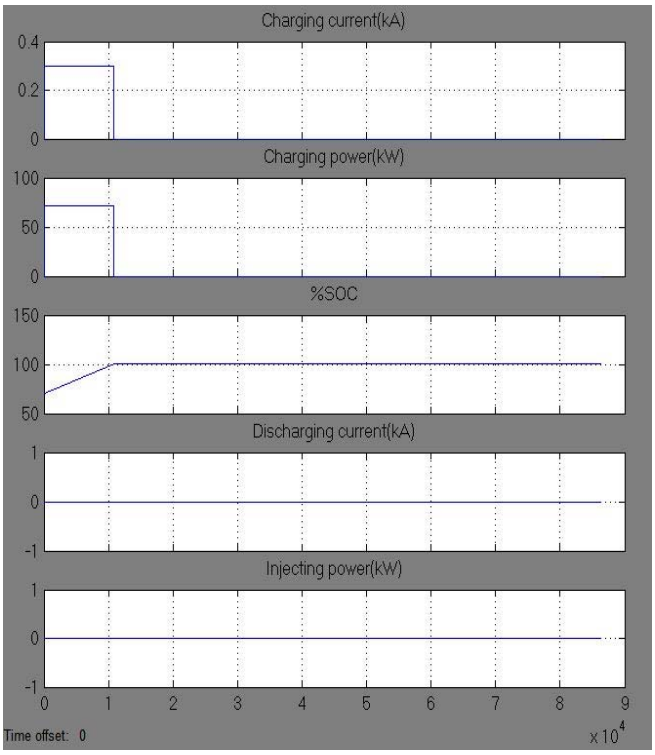

FIG. 15 BB CHARGING CURRENT (kA), CHARGING POWER (kW), PERCENTAGE OF STATE OF CHARGE, DISCHARGING CURRENT (kA) AND THEPOWER INJECTED TO THE GRID (kW) DUE TO THE DISCHARGING OF THE BATTERY ARE SHOWN ABOVE FOR THE CASE 2

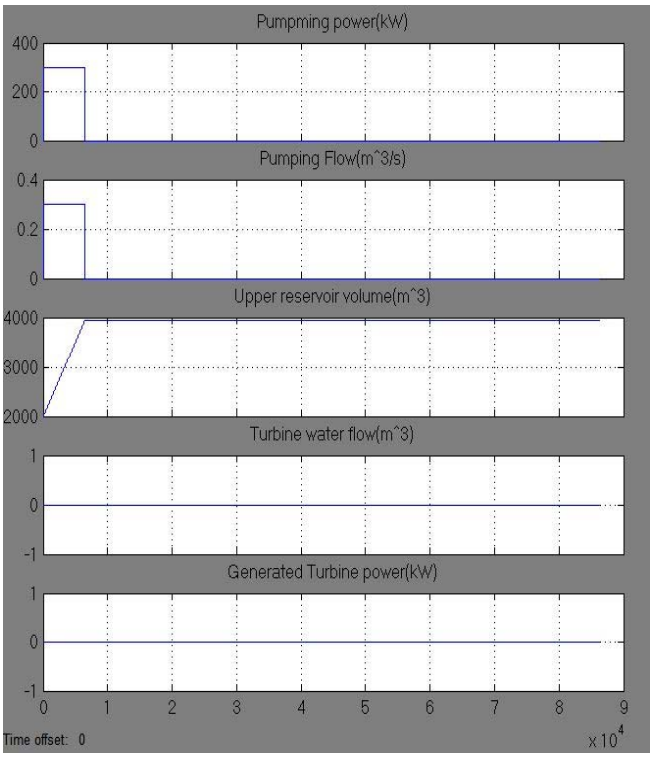

FIG. 14 PUMPING POWER (kW), PUMPING WATER FLOW RATE (m^3/s), UPPER RESERVOIR WATER VOLUME (m^3), TURBINE WATER FLOW (m^3/s) AND TURBINE GENERATED POWER (kW) FOR THE CASE 2

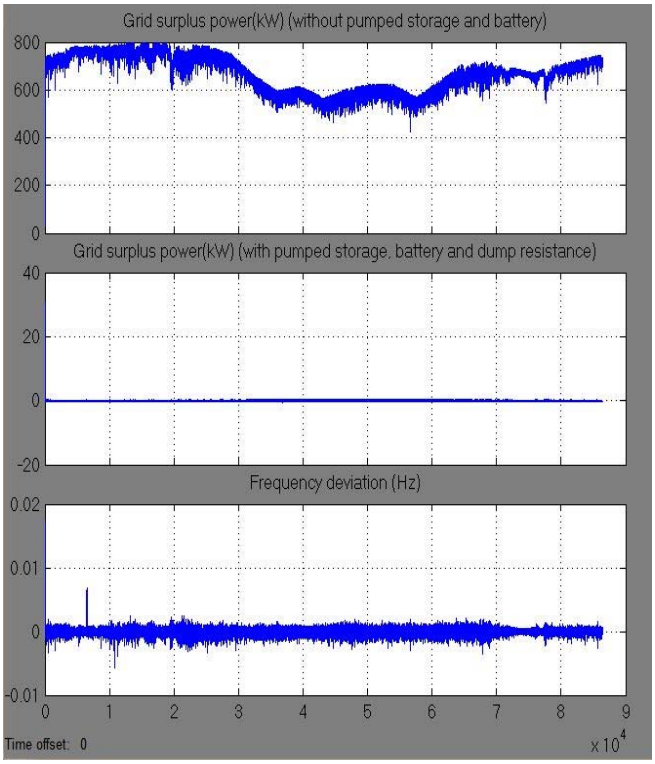

FIG. 16 GRID SURPLUS POWER (kW) WITH AND WITHOUT PUMPED STORAGE, BATTERY AND DUMP LOAD AND THE RESULTANT FREQUENCY DEVIATION ARE SHOWN ABOVE FOR THE CASE 2

DOI: 10.14355/ijes.2013.0305.05

Case 3: High Load and Low Wind

In case 3, high load and low wind speed have been used as inputs to the dynamic model to observe the outputs and system responses. Selected one day load data and wind speed are shown in FIG. 17 below.

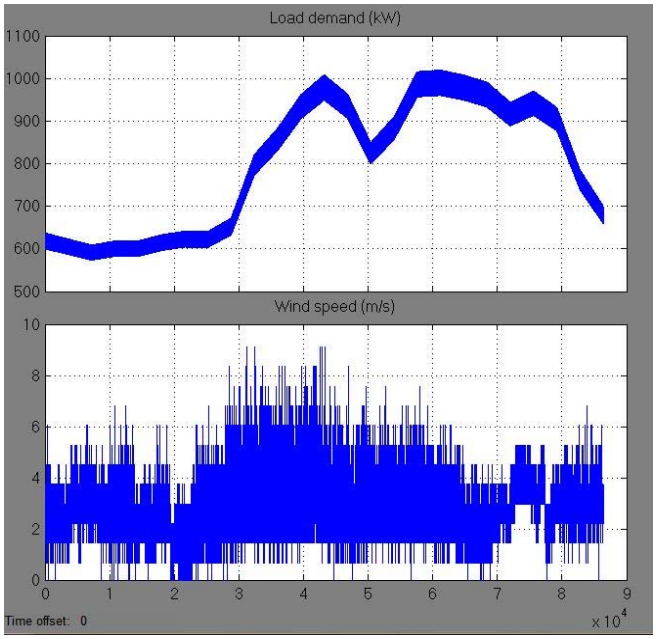

FIG. 17 LOAD DEMAND (kW) AND WIND SPEED (m/s) DATA FOR THE CASE 3

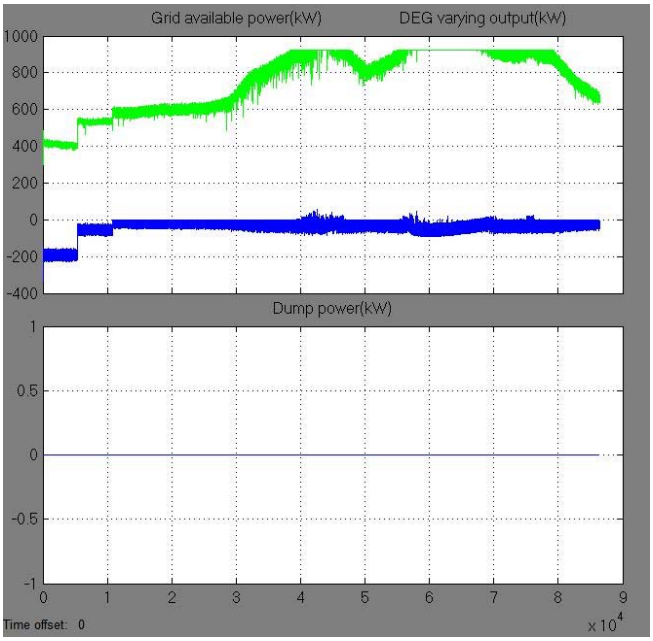

FIG. 18 IN TOP FIGURE, GRID AVAILABLE POWER (kW) AND DEG VARYING OUTPUT (kW) (FROM 400kW TO 925kW) ARE SHOWN AND IN THE BOTTOM PART DUMP POWER (kW) IS SHOWN FOR THE CASE 3

From FIG. 17 to FIG. 21 it has been observed that at first a 5500 s reservoir becomes empty and by 10000 s BB is almost discharged. This is because load is very high and WT fails to deliver enough power due to very low wind speed. DEG delivers the required amount No power dumping happening in this case. System frequency remains quite stable though two frequency dips of 0.6 Hz and 0.9 Hz are observed when load suddenly dips around 40000 s and 60000 s. Such small frequency dips are considered acceptable for remote hybrid power system.

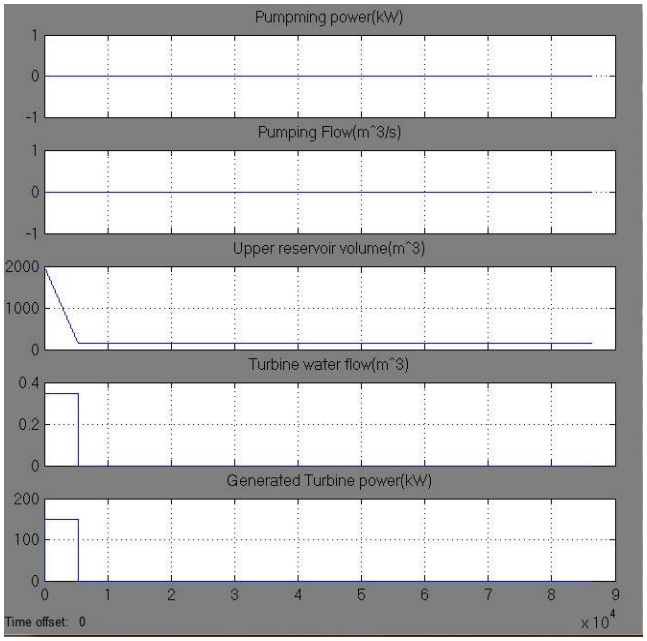

FIG. 19 PUMPING POWER (kW), PUMPING WATER FLOW (m^3/s), UPPER RESERVOIR WATER VOLUME (m^3), TURBINE WATER FLOW (m^3/s) AND TURBINE GENERATED POWER (kW) ARE SHOWN FOR THE CASE 3

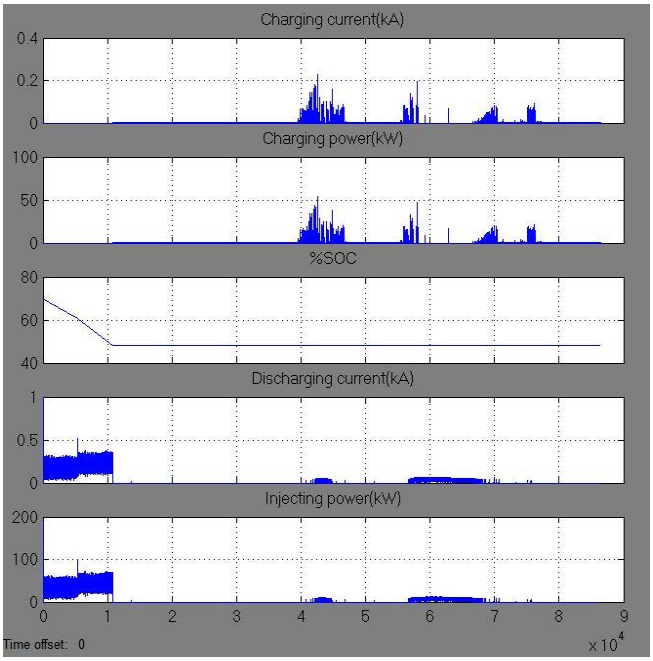

FIG. 20 CHARGING CURRENT (kA), CHARGING POWER (kW), PERCENTAGE OF STATE OF CHARGE, DISCHARGING CURRENT (kA) AND INJECTED POWER TO THE GRID (kW) DUE TO THE DISCHARGING OF THE BATTERY ARE FOR THE CASE 3

DOI: 10.14355/ijes.2013.0305.05

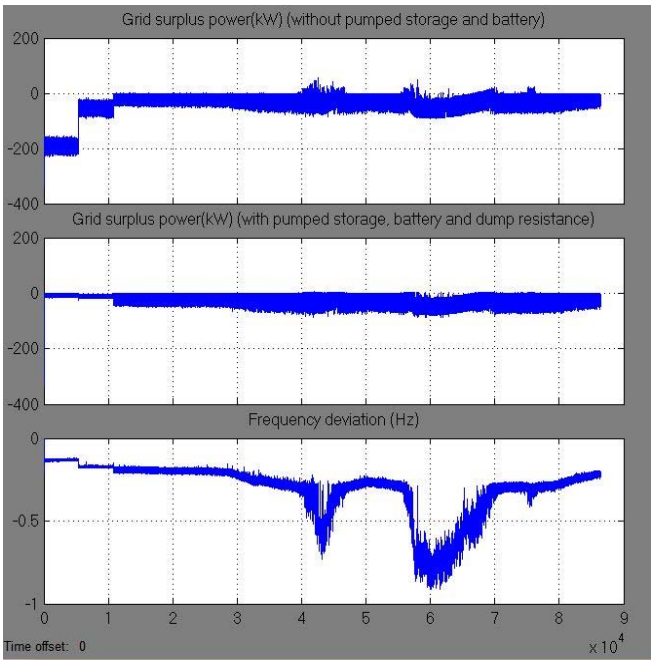

FIG. 21 GRID SURPLUS POWER (kW) WITH AND WITHOUT PUMPED STORAGE, BATTERY AND DUMP LOAD AND THE RESULTANT SYSTEM FREQUENCY DEVIATION FOR THE CASE 3

Case 4: High Load and High Wind

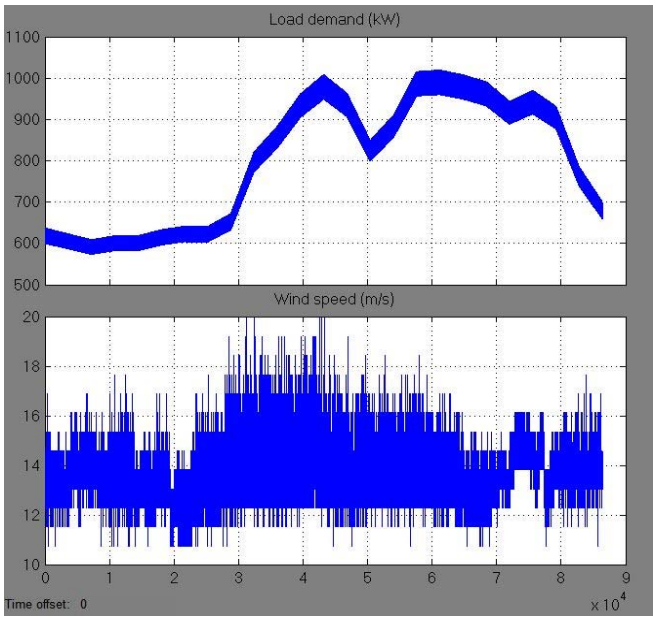

FIG. 22 LOAD DEMAND (kW) AND WIND SPEED (m/s) DATA FOR THE CASE 4

For case 4, high load and high wind speed have been used as inputs to the dynamic model and the outputs and system responses are observed. FIG. 22 shows the selected load and wind speed data for the case 4. The system simulation results are shown in the FIG. 23 to FIG. 26 below. From FIG. 22 to FIG. 26, it has been observed that in the first 7000 s reservoir becomes full and by 12000 s BB shows 100% SOC. As wind is very high, WTs generate enough power to the system so DEG delivers only 300 kW and maintains the system stability. Remaining excess power is dumped depending on the load changes. System frequency is stable for the whole time. One frequency dip of 0.4 Hz is observed at 65000 s. This happens when hydro generation turns on for a while.

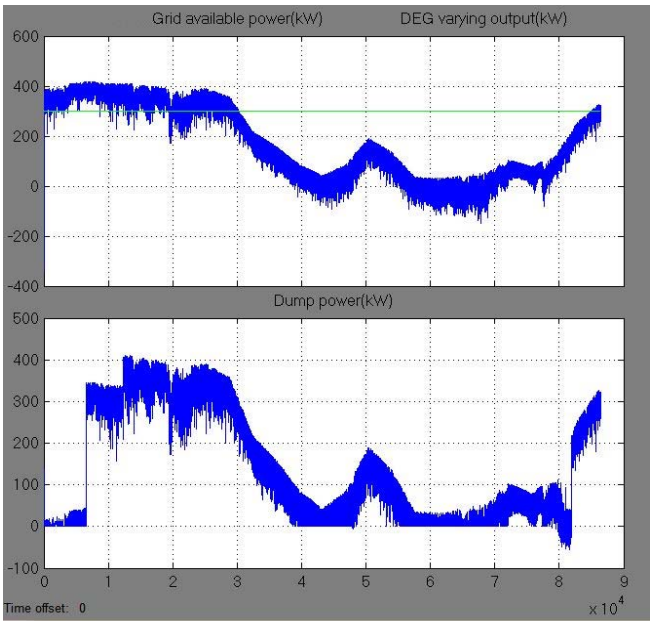

FIG. 23 IN TOP FIGURE GRID AVAILABLE POWER (kW) AND DEG OUTPUT (kW) (FLAT 300kW VALUE) ARE SHOWN AND IN THE LOWER PART DUMP POWER (kW) IS SHOWN FOR THE CASE 4

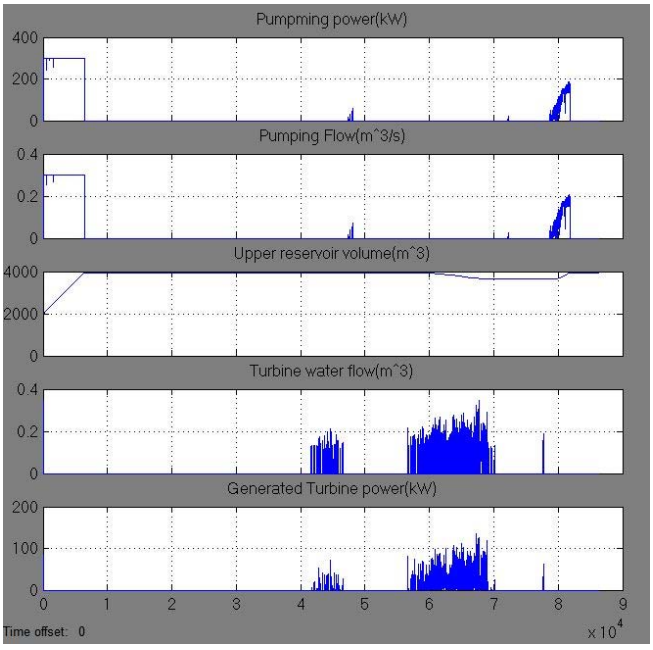

FIG. 24 PUMPING POWER (kW), PUMPING WATER FLOW (m^3/s), UPPER RESERVOIR WATER VOLUME (m^3), TURBINE WATER FLOW (m^3/s) AND TURBINE GENERATED POWER (kW) FOR THE CASE 4 ARE SHOWN ABOVE

DOI: 10.14355/ijes.2013.0305.05

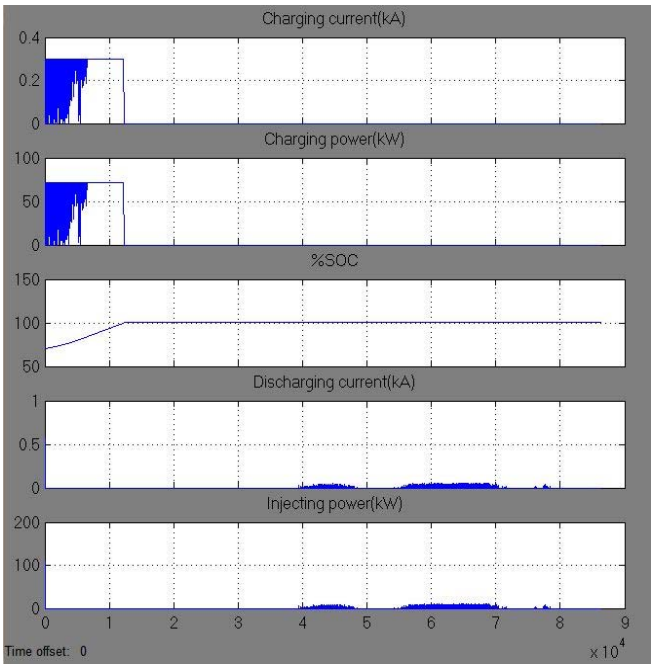

FIG. 25 CHARGING CURRENT (kA), CHARGING POWER (kW), PERCENTAGE OF STATE OF CHARGE, DISCHARGING CURRENT (kA) AND THE POWER INJECTED TO THE GRID (kW) DUE TO THE DISCHARGING OF THE BATTERY ARE SHOWN ABOVE FOR THE CASE 4

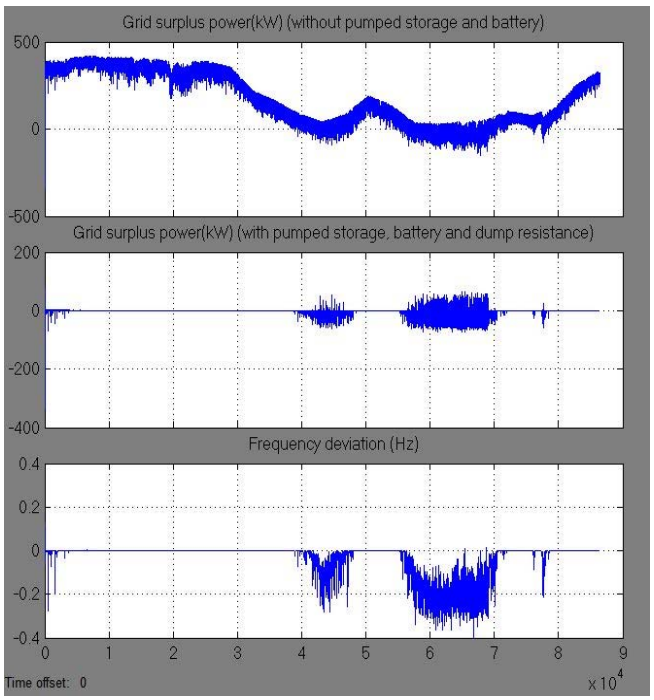

FIG. 26 GRID SURPLUS POWER (kW) WITH AND WITHOUT PUMPED STORAGE, BATTERY AND DUMP LOAD ARE SHOWN ABOVE. THE RESULTANT FREQUENCY DEVIATION IS ALSO PLOTTED FOR THE CASE 4

Case 5: Abrupt Change of Load While Wind Speed Is Steady in the Midrange

For this case study, a simple step change in the load is assumed. This case study is done to observe the system dynamics in case of a change in the load. From FIG. 26 to FIG. 31, it has been found that PWT supplies a maximum of 150 kW power for the whole time and DEG delivers the excess required amount from 200 s to 700 s. No water pumping and power dumping occur. Such sudden load change of 200 kW leads to a frequency fluctuation of 0.2 Hz that dies down in 40 s. System is capable of maintaining an almost stable frequency in such rare event.

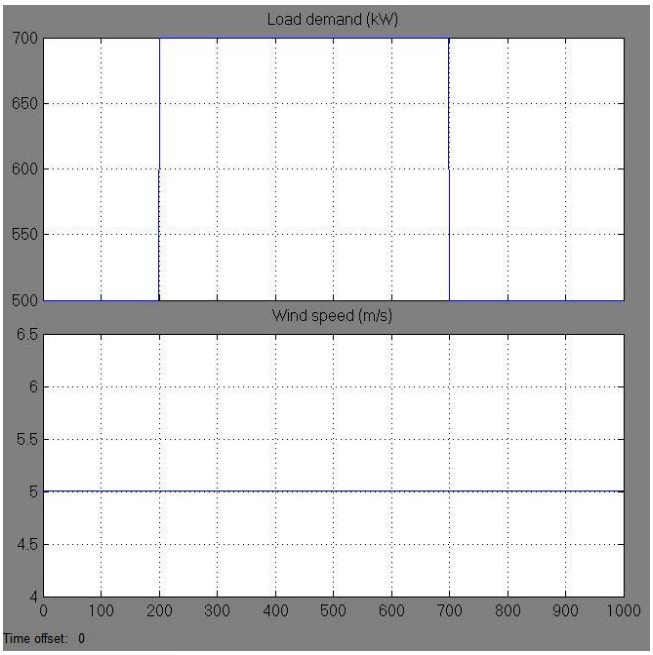

FIG. 27 LOAD DEMAND (kW) AND WIND SPEED (m/s) DATA FOR THE CASE 5

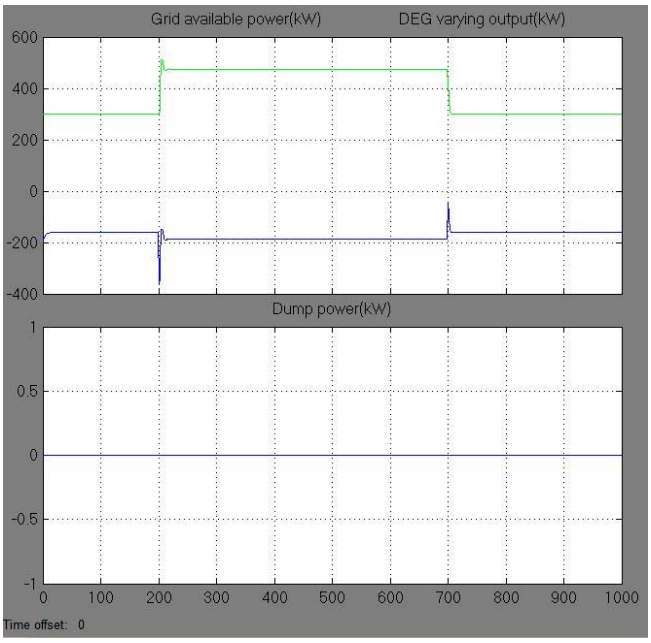

FIG. 28 IN TOP PART, GRID AVAILABLE POWER (kW) AND DEG VARYING OUTPUT (kW) (THAT CHANGES FROM 300kW TO 500kW) ARE SHOWN. IN THE LOWER PART DUMP LOAD POWER (kW) IS PLOTTED FOR THE CASE 5

DOI: 10.14355/ijes.2013.0305.05

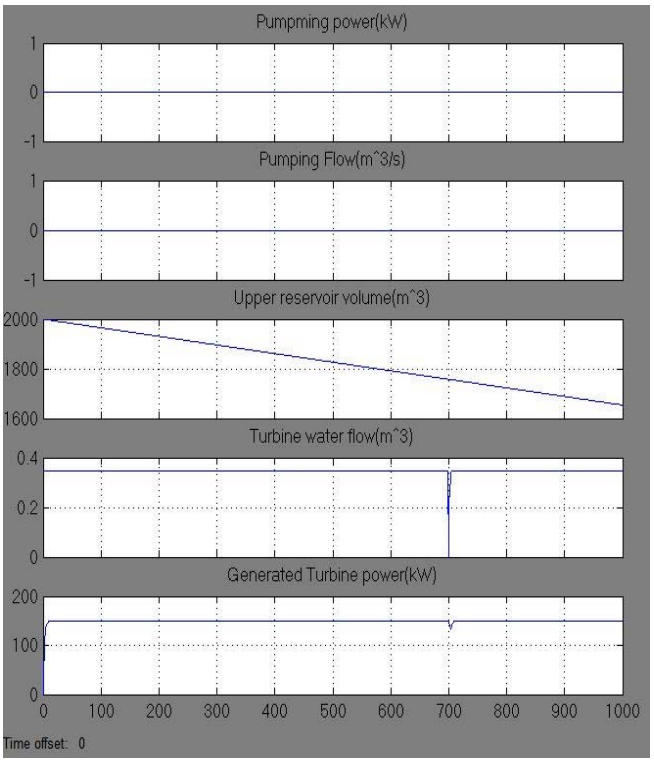

FIG. 29 PUMPING POWER (kW), PUMPING WATER FLOW (m^3/s), UPPER RESERVOIR WATER VOLUME (m^3), TURBINE WATER FLOW (m^3/s) AND TURBINE GENERATED POWER (kW) ARE PLOTTED ABOVE FOR THE CASE 5

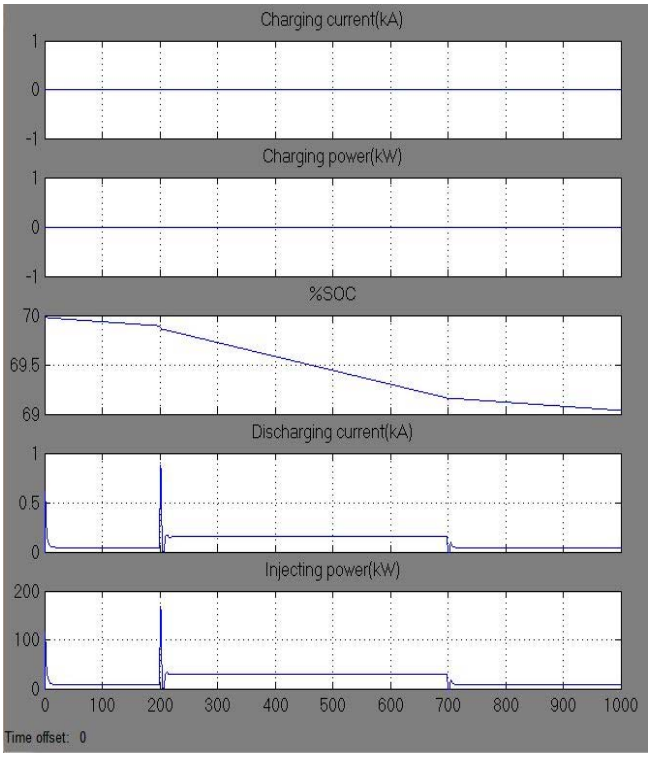

FIG. 30 BB CHARGING CURRENT (kA), CHARGING POWER (kW), PERCENTAGE OF STATE OF CHARGE, DISCHARGING CURRENT (kA) AND INJECTING POWER TO THE GRID (kW) DUE TO THE DISCHARGING OF THE BATTERY ARE PLOTTED ABOVE FOR THE CASE 5

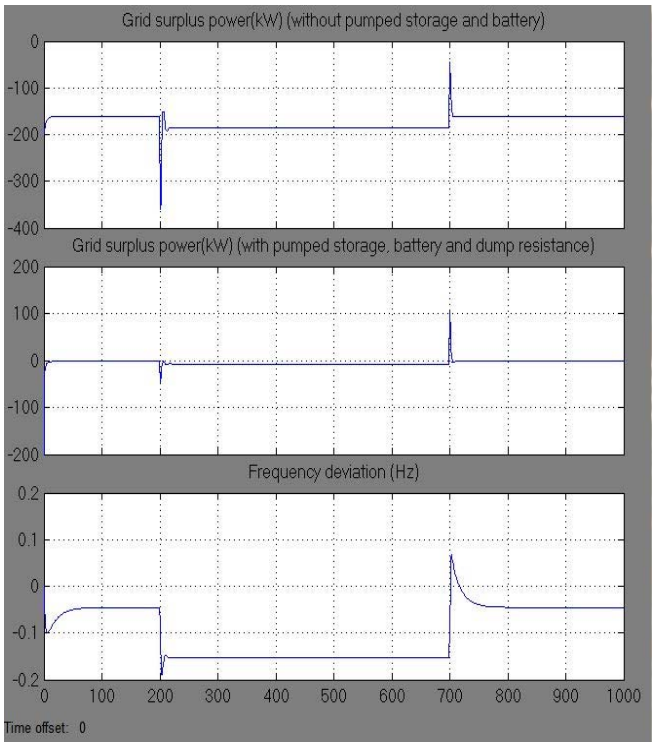

FIG. 31 THE GRID SURPLUS POWER (kW) WITH AND WITHOUT PUMPED STORAGE, BATTERY AND DUMP LOAD AND THE RESULTANT FREQUENCY DEVIATION FOR THE CASE 5

Case 6: Load Is Steady in the Midrange and Wind Speed Is Changed Abruptly

In this case study, load is a constant while wind speed is increased and then decreased. The system inputs are shown in the FIG. 32. Simulation results are shown in FIG. 32 to FIG. 36.

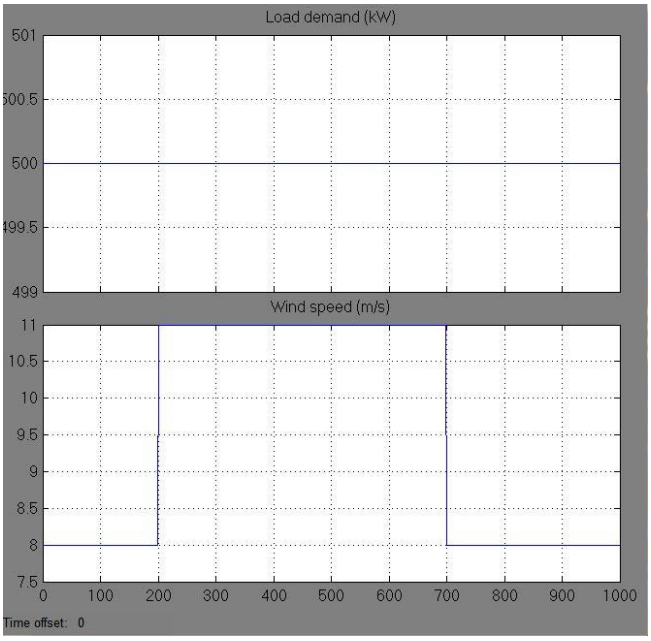

FIG. 32 LOAD DEMAND (kW) AND WIND SPEED (m/s) DATA FOR THE CASE 6

DOI: 10.14355/ijes.2013.0305.05

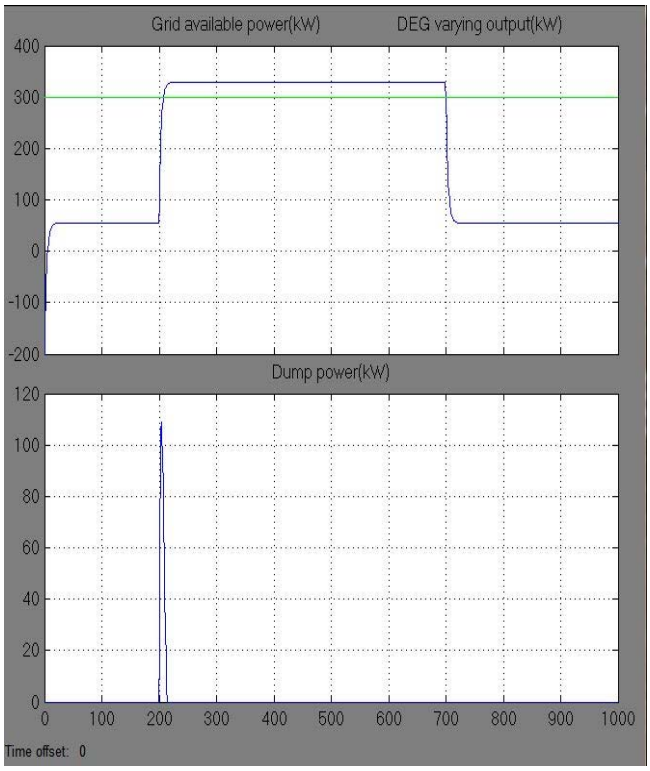

FIG. 33 IN THE TOP PART, GRID AVAILABLE POWER (kW) AND DEG VARYING OUTPUT (kW) (WITH A FLAT 300kW) AND IN BOTTOM PART DUMP POWER (kW) IS SHOWN FOR THE CASE 6

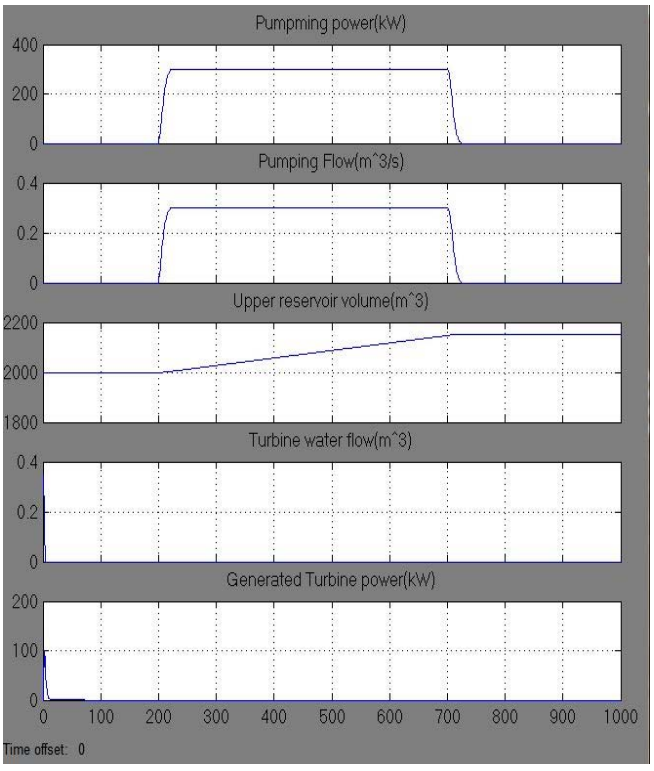

FIG. 34 PUMPING POWER (kW), PUMPING WATER FLOW (m^3/s), UPPER RESERVOIR WATER VOLUME (m^3), TURBINE WATER FLOW (m^3/s) AND TURBINE GENERATED POWER (kW) ARE SHOWN ABOVE FOR THE CASE 6

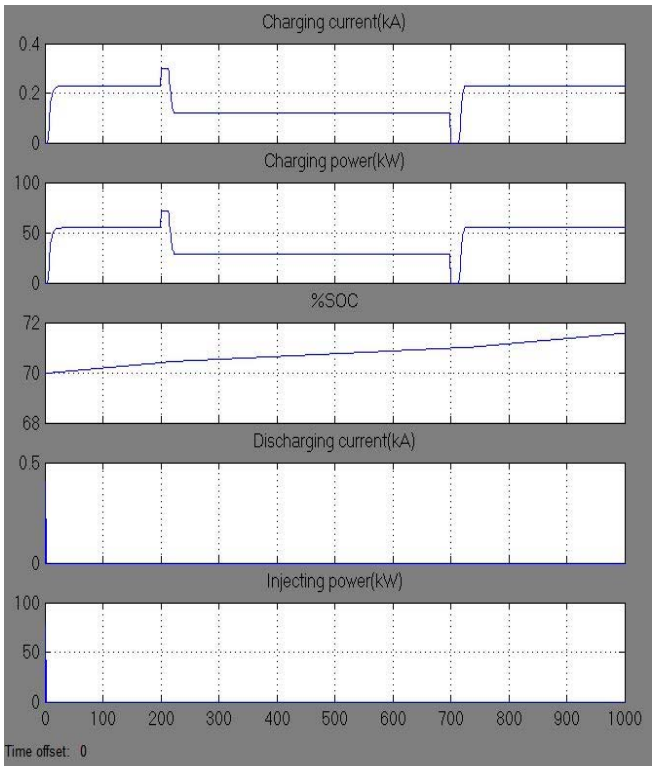

FIG. 35 CHARGING CURRENT (kA), CHARGING POWER (kW), PERCENTAGE OF STATE OF CHARGE, DISCHARGING CURRENT (kA) AND INJECTED POWER TO THE GRID (kW) DUE TO THE DISCHARGING OF THE BATTERY ARE PLOTTED ABOVE FOR THE CASE 6

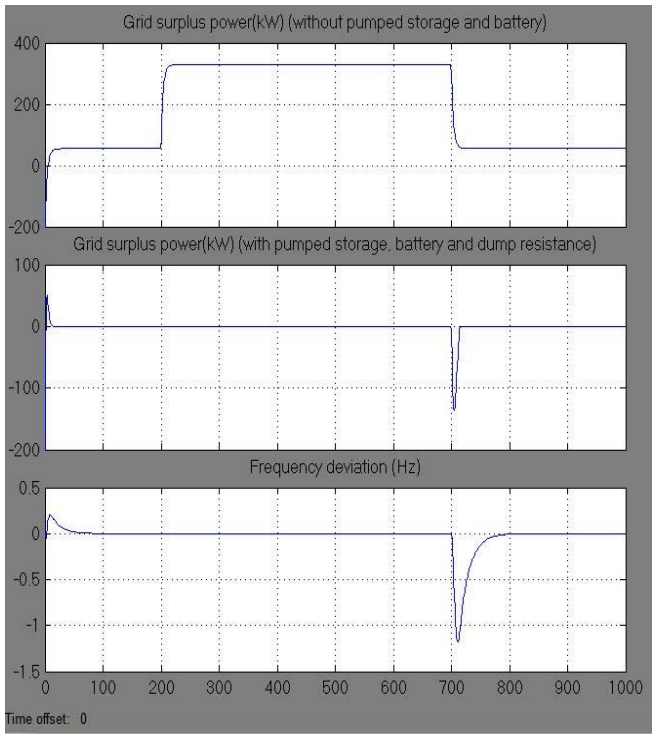

FIG. 36 GRID SURPLUS POWER (kW) WITH AND WITHOUT PUMPED STORAGE, BATTERY AND DUMP RESISTANCE AND THE RESULTANT FREQUENCY DEVIATION ARE SHOWN ABOVE FOR THE CASE 6

DOI: 10.14355/ijes.2013.0305.05

From FIG. 31 to FIG. 36, it has been found that as wind speed increases, the water pumping starts and operates of its maximum rating from t=200 s to 700 s. BB charges as well for a while. DEG supplies 300 kW all time.

At 700 s, a sudden 1.1 Hz system frequency dip is found when wind speed drops from to 8 m/s from 11 m/s. Such a large dip may not be acceptable. But a sudden wind speed drop of 3 m/s is impossible. This case study shows that the proposed supervisory controller is capable of controlling the system in extreme conditions.

All above discussed 6 cases show almost steady system frequency for extreme conditions. These are extreme situations for the load demand and wind speed data in a year. Real situations may be much milder than above selected cases.

Conclusions

This paper presented a dynamic simulation model and a supervisory controller for a remote hybrid power system with a proposed pumped hydro storage. From the simulation results, based on six possible extreme cases, it can be concluded a) a minimum of 300 kW operation of DEG permits higher penetration of wind energy and leads to a low diesel consumption and maintains a fairly stable system frequency b) proposed dump load addition will prevent the system frequency spikes in high wind and make the system operation easier and result in less frequency deviations. Expected response of pump hydro system with battery storage is acceptable for a remote location like Ramea Island. Simulation of the presented dynamic model with proposed PHS, BB and dump load is significantly fast. Using a 0.01 s time step, a day i.e. 86400s simulation takes about 30 min to complete on a computer with Intel Core2Duo 2.1 GHz processor. The system model presented in this paper includes all real world characteristics curves, nonlinear efficiencies, losses and a supervisory controller. Moreover, this model can be used to check system stability and be modified easily for possible future extension to the hybrid power system. Wind data and load data of any day can be used with the model to determine the system expected response. This model allows us to simulate few months of operations of Ramea hybrid system and study parameters such as fuel consumption. Such a study is not possible in any commercially available software. Incorporating higher order complicated system components models in the blocks of this model can improve this model but that will considerably increase the simulation time. As a future work, system AC voltage analysis can be done to observe the voltage variations in the system.

ACKNOWLEDGMENT

Authors thank The Wind Energy Strategic Network (WESNet) (which is a Canada wide research network, funded by industry and the Natural Sciences and Engineering Research Council of Canada (NSERC)) for funding this research.

REFERENCES

[1] Introduction to the Ramea Island, [Online]. Available: http://www.ramea.ca/. [Accessed 30-01-2013].

[2] CANMET Energy, "Natural Resource Canada," Natural Resource Canada, 07-07-2007. [Online].Available: http://canmetenergy.nrcan.gc.ca/renewables/wind/464. [Accessed 30-01-2013].

[3] M. Oprisan, "IEA Wind," IEA Wind – KWEA Joint Workshop, 01-04-2007. [Online].Available: http://www.ieawind.org/wnd_info/KWEA_pdf/Oprisan_KWEA_.pdf. [Accessed 30 01 2013].

[4] T. Iqbal, "Feasibility Study of Pumped Hydro Energy Storage for Ramea Wind-Diesel Hybrid Power System," The Harris Centre, St. John's, 2009.

[5] D.-J. Lee and L. Wang, "Small-Signal Stability Analysis of an Autonomous Hybrid Renewable Energy Power Generation/Energy Storage System Part I: Time-Domain Simulations," IEEE TRANSACTIONS ON ENERGY CONVERSION, vol. 23, no. 1, pp. 311-320, 2008.

[6] Md. Rahimul Hasan Asif and Tariq Iqbal, "A novel method to model a hybrid power system with pumped hydro storage for Ramea, Newfoundland", IEEE, Newfoundland Electrical and Computer Engineering Conference, St. John's, 2012

[7] A. G. Rodríguez, A. G. Rodríguez and M. B. Payán, "Estimating Wind Turbines Mechanical Constants," in INTERNATIONAL CONFERENCE ON RENEWABLE ENERGIES AND POWER QUALITY (ICREPQ'07), Bilbao, 2007.

[8] Windmatic, "Windmatic 15s," [Online]. Available: http://windmatic.com/15s-brochure.pdf. [Accessed 30 01 2013].

DOI: 10.14355/ijes.2013.0305.05

[9] Northern Power Systems, "Northern Power 100," [Online]. Available: http://www.northernpower.com/pdf/NPS100-21_SpecSheet_EU-A4_English_2012.pdf. [Accessed 10 01 2013].

[10] Advantica Inc., "Moment of Inertia and Pump Startup/Failure," 14 03 2011. [Online].Available: http://my.advanticagroup.com/support/allsecure/watersecure/releases_advisories/KBA_pump_moment_of_inertia.pdf. [Accessed 30 01 2013].

[11] "The Engineering Toolbox," [Online]. Available: http://www.engineeringtoolbox.com/minor-loss-coefficients-pipes-d_626.html. [Accessed 30 01 2013].

[12] G. Brown, "Henry Darcy and His Law," 22 06 2000. [Online]. Available: http://biosystems.okstate.edu/darcy/index.htm. [Accessed 30 01 2013].

[13] Renewables First, "Pelton & Turgo Turbines," Renewables First, [Online]. Available: http://www.renewablesfirst.co.uk/pelton-and-turgo-turbines.html. [Accessed 30 01 2013].

[14] Chen, H., Cong, T., Yang, W., Tan, C., Li, Y., and Ding, Y., Progress in electrical energy storage system: a critical review. Progress in Natural Science 19 (2008), 291–312.